Near-to-far-field spectral evolution in a plasmonic crystal: Experimental verification of the equipartition of diffraction orders

D. J. Park,[1] K. G. Lee,[1] H. W. Kihm,[1] Y. M. Byun,[1] D. S. Kim,[1,a)] C. Ropers,[2] C. Lienau,[3] J. H. Kang,[4] and Q-Han Park[4]
[1]*Department of Physics and Astronomy, Seoul National University, 151-747 Seoul, Republic of Korea*
[2]*Max-Born Institute für Nichlineare Optik und Kurzeitspektroskopie, D-12489 Berlin, Germany*
[3]*Carl von Ossietzky Universität, Institut für Physik, D-26111 Oldenburg, Germany*
[4]*Department of Physics, Korea University, 136-701 Anam-dong, Sungbuk-Gu, Seoul, Republic of Korea*

(Received 21 January 2008; accepted 4 June 2008; published online 20 August 2008)

We report on drastic changes in the near-field spectrum as it evolves into the far field in periodically corrugated metallic nanoslit arrays. The far-field spectral minimum is located exactly at the near-field spectral maximum, where a quasimonochromatic standing wave pattern is observed in the near field. These results are in excellent agreement with the equipartition of diffraction orders recently proposed [K. G. Lee and Q-Han Park, Phys. Rev. Lett. **95**, 103902 (2005)]. © *2008 American Institute of Physics*. [DOI: 10.1063/1.2951587]

Characterizing strongly localized electromagnetic fields on a corrugated metal surface has become an important issue not only from a fundamental science point of view but also from the technological side. Diverse areas such as enhanced transmission,[1] negative index of refraction materials,[2] superlensing,[3] biosensing,[4] near-field fabrication,[5] and optical nanoantennas[6] require a detailed knowledge of both spatial and spectral near-field profiles.[7]

In atomic, excitonic[8] or single plasmonic particles,[9] their electromagnetic near-field profile gives valuable information on the homogeneous spectral linewidth as well as on the localization of wavefunctions. In these systems, the near-field profiles differ mainly in intensity in comparison to the far-field, but not in their spectral shapes—at least not in homogeneously broadened systems. In periodic arrays of nano-holes,[1,10] nanoslits[11] and nanoparticle,[12] however, the periodicity provides another length-scale different from the particle size, which can decide whether a particular wavelength component is mainly evanescent or propagating. In using plasmonic crystals in applications such as plasmonic waveguiding,[13] biosensing,[14] and surface enhanced Raman scattering, any spectroscopic difference between near and far field has important technological implications.

In this letter, we report on the near-to-far field spectral evolution in a one-dimensional plasmonic crystal. We experimentally decompose the near-field spectrum of this system into its evanescent and propagating components. By mapping near-field spatial profiles with subwavelength resolution, we confirm that at the peak of the near-field intensity, all of the diffraction orders are suppressed to almost zero except for the first order, which leads to the formation of a standing wave pattern. Such a behavior has recently been predicted theoretically by Lee and Park in terms of the *equipartition of diffraction orders*.[15] Our experiments show that the near-field spectral information is crucial in determining surface electromagnetic field profile, while resolving the controversial issue of the *negative* role of surface plasmons.[16]

A nanoslit array is prepared by electron beam lithography on a 78 nm thick gold film thermally evaporated on a 320 μm thick sapphire substrate. The periodicity of the array is measured by Bragg diffraction and also by scanning electron microscopy [inset of Fig. 1(a)], and is found to be $d=761$ nm. The slit width a is approximately 100 nm. Measurements of the near-to-far evolution of the transmission spectra are performed by employing a collection mode near-field scanning optical microscope using a metal-coated aperture probe with a 100 nm aperture diameter (Nanonics Imaging, Ltd.). In these measurements, the tip-to-sample distance z is varied between 0–100 μm and the incident wavelength is scanned between 740 and 840 nm using a tunable Ti: sapphire laser [Fig. 1(a)]. The far-field spectrum is recorded using a tungsten lamp [Fig. 1(b)] for comparison with the near-field experiments. A clear transmission dip is seen at the surface plasmon polariton (SPP) resonance, which is determined by the period d as $\lambda_{sp}=d\sqrt{\varepsilon_m/(\varepsilon_m+1)} \approx 780$ nm. Here ε_m denotes the gold dielectric function.[17] This *negative* role of surface plasmons on the far-field transmission has been predicted numerically[16] and explained theoretically in terms of an "antiresonance"[16] or equipartition of diffraction orders.[15] Evidently, the effect of the slits is to couple the incident light field to different evanescent SPP orders. For infinitely small slits, the coupling efficiency is the same for all orders, as it is essentially given by the overlap integral of the incident and SPP fields evaluated over the slit width. This equality of the coupling efficiencies has recently

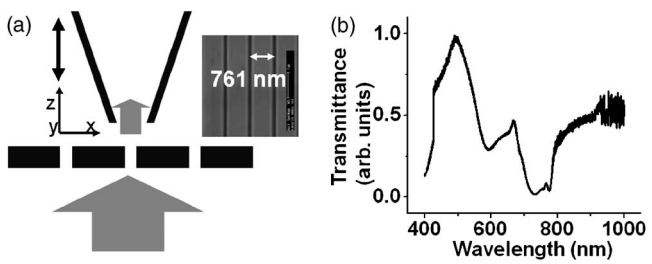

FIG. 1. (a) Schematic diagram of the experimental setup. (inset) scanning electron microscope image of the nanoslit array. (b) Far-field transmission spectrum recorded by using a tungsten white light lamp.

a)Author to whom correspondence should be addressed. Electronic mail: dsk@phya.snu.ac.kr.

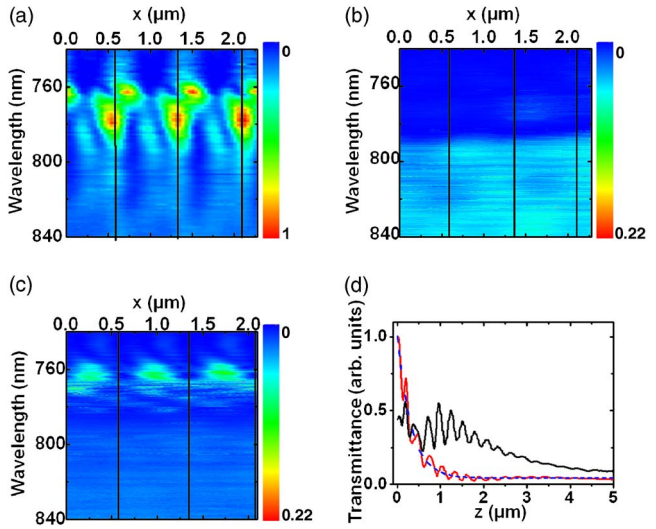

FIG. 2. (Color online) (a) Experimental near-field spatial profile $I(x,z=0,\lambda)$ as a function of excitation wavelength. (b) Intensity profile $I(x,z=100\ \mu\text{m},\lambda)$ at a tip-sample distance of $z=100\ \mu$m. (c) $I(x,z=3\ \mu\text{m},\lambda)$. Black solid line denotes slit positions. (d) Distance-dependence of the transmission near the slit center $I(z,\lambda)$ at different excitation wavelengths of $\lambda=761$ nm (black curve), $\lambda=780$ nm (red curve), and exponential fitting for case of excitation wavelength $\lambda=780$ nm. (blue dotted curve). For each case the average intensity over one period d is taken.

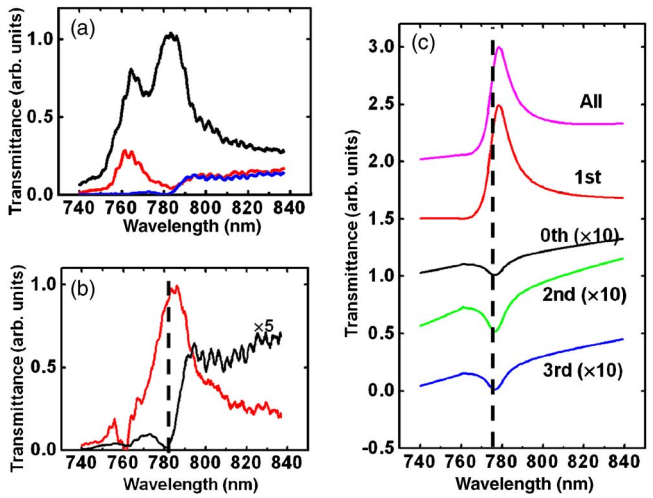

FIG. 3. (Color online) (a) Spatially integrated spectrum $\bar{I}(z,\lambda)=\int I(x,z,\lambda)dx$ as a function of tip-sample distance z. The black curve denotes the near-field spectrum, red curve gives $\bar{I}(3\ \mu\text{m},\lambda)$ and the blue curve $\bar{I}(100\ \mu\text{m},\lambda)$. (b) Evanescent near field spectrum $\bar{I}_{ev}(\lambda)=\bar{I}(0,\lambda)-a\cdot\bar{I}(3\ \mu\text{m},\lambda)$ obtained by subtracted the propagating components. The normalization was chosen so as to minimize the contribution from propagating components. (b) Calculated near-field spectrum together with 0^{th} order (black curve), first order (red curve), second order (green curve), and third order (blue curve) diffraction. The transmittances of the 0^{th}, second, and third orders are magnified by a factor of 10.

been termed equipartition of diffraction orders.[15] The transmission and reflection then result from this constant coupling efficiency for each diffraction order, multiplied by a suitable resonance factor. Therefore if one SPP mode is excited on resonance, the transmission and the reflection of all other modes, including the zero order mode propagating into the far field, must vanish.[13] In our near-to-far-field measurement, this predicted behavior shows up clearly as we measure the spectrum by varying the tip-to-surface distance.

Figure 2(a) shows a contour plot of the near-field spatial profile as a function of the excitation wavelength. The near-field intensity is brightest near the flat-metal surface plasmon wavelength $\lambda_{sp}=$ nm This is also the wavelength at which a standing wave pattern is most pronounced. The maxima of the spatial intensity lie at the slit opening region due to the additional contribution of direct transmission. Around the Rayleigh wavelength $\lambda_R=d=761.3$ nm another region of relative brightness occurs. In the far-field data shown in Fig. 2(b) at $z=100\ \mu$m both these peak wavelength regions die out, together with any standing wave pattern: the spatial pattern is essentially homogeneous. For $\lambda\geqslant\lambda_R$, only the 0^{th} order diffraction survives into the far field.[18] For shorter wavelengths, the orders 0 and ±1 propagate. Here, the finite dimension of the slit sample of about 100 μm causes a finite spread in k vectors, resulting in a vanishing interference pattern at large distances. In addition, the wavelength region of maximum near-field intensity ($760\ \text{nm}\leqslant\lambda\leqslant780$ nm) becomes a region of minimum intensity in the far field, suggesting a substantial difference between the near and far-field spectra. In an intermediate region, $z\sim3\ \mu$m [Fig. 2(c)], the peak around λ_R is still present and the maxima lies between the slit, which support that the constructive interference of ±1 diffraction orders result in this peak. On the other hand, the peak at λ_{sp} is now completely suppressed.

Figures 2(a) and 2(c) imply that different spectral components have very different z dependencies. For two representative spectral components, $\lambda=761$ nm (black curve) and 780 nm (red curve), this dependence is shown in Fig. 2(d). Except for small oscillations due to Fabry–Perot-like interferences between tip and sample, the profile for $\lambda=780$ nm decays exponentially, with a decay length of about 330 nm (blue dotted line). This is in good agreement with the theoretical decay length of $\lambda/4\pi/\sqrt{\lambda^2/d^2-1}=297$ nm for the first order evanescent component. In contrast, the profile for 761 nm shows, in addition to the initial exponential decay, a component persisting for about 2 μm. This slowly decaying component reflects the contribution from the propagating first diffraction order, grazing along the surface.

Figure 3(a) shows spectra integrated along the x axis for $z=0\ \mu$m (black curve), 3 μm (red curve), and 100 μm (blue curve). Subtracting the $z=100\ \mu$m data from those at $z=3\ \mu$m gives the propagating first diffraction order component. Now, in the next step, we subtract the first-order diffraction spectrum from the near-field data. The resulting, purely evanescent spectral component is shown in Fig. 3(b), together with the far-field component. We emphasize that the near-field *maximum* lies at λ_{sp} and coincides with the *minimum* of the far-field spectrum.

To explain the different z dependencies of these spectral components, we performed a calculation based on a diffraction order expansion[19] combined with matching boundaries at the metal-dielectric interface by using the surface impedance boundary condition.[15,20] Figure 3(c) shows the near-field intensity obtained by summing all diffraction orders (top curve), together with the first to third diffraction orders. The first order diffraction order alone captures most of the essential features of the full calculation, both qualitatively and quantitatively, demonstrating that for wavelengths larger than the grating period, the near-field spectrum is dominated by the evanescent first diffraction order. Only the first diffraction order shows a maximum near λ_{sp}, while all other orders show minima at this wavelength, in agreement with

the experimental observations. This difference is expected in terms of the equipartition of diffraction orders[15] and the suppression of the 0^{th} order has been referred to as the *negative role of surface plasmons.*[16] It is evident that the role of surface plasmon is negative only in so far as the far-field transmittance is of primary concern. Clearly, the near-field intensity of the first diffraction is largest, so that one may say that SPPs play a *positive* role, enhancing the near-field intensity.

In conclusion, we have shown drastically different near field and far-field transmission spectra of metal nanoslit arrays. In the near field, the evanescent first diffraction order dominates, giving rise to an intensity maximum near the SPP resonance λ_{sp}. Other diffraction orders are suppressed. In the far field, however, the transmission spectrum shows a minimum at the near the SPP resonance. This behavior can be qualitatively explained by the equipartition of diffraction orders, expected for nanoslit gratings with vanishing slit width. Our experiments clarify the positive and negative roles of surface plasmon polaritons in such arrays: in terms of the far-field transmission, SPP excitation plays a negative role, suppressing the transmission near the SPP resonance. Yet, it clearly enhances the near field intensity in this wavelength region. Our results provide new insight into the spectral properties of optical near fields in metallic nanostructures and resolve a partly controversial about the role of SPP for the transmission of light through such gratings.[21]

Financial support of the work in Korea by Korean Government (MOST, MOEHRD) through KRF (Grant Nos. C00012 and C00032), KOSEF, Seoul R&D program and Nano R&D program (Grant No. 2007-02939), and that in Germany by the DFG (SF296) is gratefully acknowledged. The authors thank Sang mo Chun for advice on the theoretical simulations, Minah Seo for discussions and artwork for the figures, and also Joong-Wook Lee for many valuable discussions.

[1]T. W. Ebbesen, H. J. Lezec, H. F. Ghaemi, T. Thio, and P. A. Wolff, Nature (London) **391**, 667 (1998).
[2]J. B. Pendry and S. A. Ramakrishna, J. Phys.: Condens. Matter **15**(37), 6345 (2003); R. Moussa, S. Foteinopoulou, L. Zhang, G. Tuttle, K. Guven, E. Ozbay, and C. M. Soukoulis, Phys. Rev. B **71**, 085106 (2005); S. Anantha Ramakrishna, Rep. Prog. Phys. **68**, 449 (2005); N. Fang and X. Zhang, Appl. Phys. Lett. **82**, 161 (2003); S. Linden, C. Enkrich, M. Wegener, J. Zhou, T. Koschny, and C. M. Soukoulis, Science **306**, 1351 (2004).
[3]Z. Liu, S. Durant, H. Lee, Y. Xiong, Y. Pikus, C. Sun, and X. Zhang, Opt. Lett. **32**, 629 (2007).
[4]S. Ekgasit, C. Thammacharoen, F. Yu, and W. Knoll, Anal. Chem. **76**, 2210 (2004); J. Homola, S. S. Yee, and G. Gauglitz, Sens. Actuators B **54**, 3 (1999).
[5]Z. W. Liu, Q. H. Wei, and X. Zhang, Nano Lett. **5**, 957 (2005).
[6]P. Muehlschlegel, H. J. Eisler, O. J. F. Martin, B. Hecht, and D. W. Pohl, Science **308**, 1607 (2005).
[7]M. A. Seo, A. J. L. Adam, J. H. Kang, J. W. Lee, S. C. Jeoung, Q. H. Park, P. C. M. Planken, and D. S. Kim, Opt. Express **15**, 11781 (2007).
[8]S. K. Eah, W. Jhe, and Y. Arakawa, Appl. Phys. Lett. **80**, 2779 (2002); E. Runge and C. Lienau, Phys. Rev. B **71**, 035347 (2005); K. Matsuda, T. Saiki, S. Nomura, M. Mihara, Y. Aoyagi, S. Nair, and T. Takagahara, Phys. Rev. Lett. **91**, 177401 (2003).
[9]T. Klar, M. Perner, S. Grosse, G. Von Plessen, W. Spirkl, and J. Feldmann, Phys. Rev. Lett. **80**, 4249 (1998).
[10]L. Martin-Moreno, F. J. Garcia-Vidal, H. J. Lezec, K. M. Pellerin, T. Thio, J. B. Pendry, and T. W. Ebbesen, Phys. Rev. Lett. **86**, 1114 (2001).
[11]J. A. Porto, F. J. Garcia-Vidal, and J. B. Pendry, Phys. Rev. Lett. **83**, 2845 (1999); I. R. Hooper and J. R. Sambles, Phys. Rev. B **65**, 165432 (2002); F. J. Garcia-Vidal, H. J. Lezec, T. W. Ebbesen, and L. Martin-Moreno, Phys. Rev. Lett. **90**, 213901 (2003); A. Nahata, R. A. Linke, T. Ishi, and K. Ohashi, Opt. Lett. **28**, 423 (2003); S. Young-Min, S. Jin-Kyu, J. Kyu-Ha, W. Jong-Hyo, S. Anurag, and P. Gun-Sik, Phys. Rev. Lett. **99**, 147402 (2007).
[12]S. Linden, J. Kuhl, and H. Giessen, Phys. Rev. Lett. **86**, 4688 (2001); Z. H. Kim and S. R. Leone, J. Phys. Chem. B **110**, 19804 (2006).
[13]S. A. Maier, M. D. Friedman, P. E. Barclay, and O. Painter, Appl. Phys. Lett. **86**, 071103 (2005); H. S. Won, K. C. Kim, S. H. Song, C.-H. Oh, P. S. Kim, S. Park, and S. I. Kim, Appl. Phys. Lett. **88**, 011110 (2006); J. J. Ju, S. Park, M.-s Kim, J. T. Kim, S. K. Park, Y. J. Park, and M.-H. Lee, Appl. Phys. Lett. **91**, 171117 (2007).
[14]J. J. Baumberg, T. A. Keif, Y. Sugawara, S. Cintra, M. E. Abdelsalam, P. N. Bartlett, and A. E. Russell, Nano Lett. **5**, 2262 (2005).
[15]K. G. Lee and Q. H. Park, Phys. Rev. Lett. **95**, 103902 (2005).
[16]Q. Cao and P. Lalanne, Phys. Rev. Lett. **88**, 057403 (2002).
[17]P. B. Johnson and R. W. Christy, Phys. Rev. B **6**, 4370 (1972).
[18]S. C. Hohng, Y. C. Yoon, D. S. Kim, V. Malyarchuk, R. Mueller, C. Lienau, J. W. Park, K. H. Yoo, J. Kim, H. Y. Ryu, and Q. H. Park, Appl. Phys. Lett. **81**, 3239 (2002); D. S. Kim, S. C. Hohng, V. Malyarchuk, Y. C. Yoon, Y. H. Ahn, K. J. Yee, J. W. Park, J. Kim, Q. H. Park, and C. Lienau, Phys. Rev. Lett. **91**, 143901 (2003).
[19]L. Rayleigh, Proc. R. Soc. London, Ser. A **79**, 532 (1907).
[20]Hans L. and R. Depine, Appl. Opt. **32**, 3459 (1993).
[21]H. J. Lezec and T. Thio, Opt. Express **12**, 3629 (2004).